





Article

Mapping Habitat Structures of Endangered Open Grassland Species (*E. aurinia*) Using a Biotope Classification Based on Very High-Resolution Imagery

Steffen Dietenberger ^{1,*} , Marlin M. Mueller ¹ , Andreas Henkel ², Clémence Dubois ¹ , Christian Thiel ¹ 
and Sören Hese ³

¹ Institute of Data Science, German Aerospace Center (DLR), Mälzerstraße 3-5, 07745 Jena, Germany

² Nature Protection and Research, Hainich National Park Administration, Bei der Marktkirche 9, 99947 Bad Langensalza, Germany

³ Department of Earth Observation, Institute of Geography, Friedrich Schiller University Jena, Leutragraben 1, 07743 Jena, Germany

* Correspondence: steffen.dietenberger@dlr.de

Abstract: Analyzing habitat conditions and mapping habitat structures are crucial for monitoring ecosystems and implementing effective conservation measures, especially in the context of declining open grassland ecosystems in Europe. The marsh fritillary (*Euphydryas aurinia*), an endangered butterfly species, depends heavily on specific habitat conditions found in these grasslands, making it vulnerable to environmental changes. To address this, we conducted a comprehensive habitat suitability analysis within the Hainich National Park in Thuringia, Germany, leveraging very high-resolution (VHR) airborne, red-green-blue (RGB), and color-infrared (CIR) remote sensing data and deep learning techniques. We generated habitat suitability models (HSM) to gain insights into the spatial factors influencing the occurrence of *E. aurinia* and to predict potential habitat suitability for the whole study site. Through a deep learning classification technique, we conducted biotope mapping and generated fine-scale spatial variables to model habitat suitability. By employing various modeling techniques, including Generalized Additive Models (GAM), Generalized Linear Models (GLM), and Random Forest (RF), we assessed the influence of different modeling parameters and pseudo-absence (PA) data generation on model performance. The biotope mapping achieved an overall accuracy of 81.8%, while the subsequent HSMs yielded accuracies ranging from 0.69 to 0.75, with RF showing slightly better performance. The models agree that homogeneous grasslands, paths, hedges, and areas with dense bush encroachment are unsuitable habitats, but they differ in their identification of high-suitability areas. Shrub proximity and density were identified as important factors influencing the occurrence of *E. aurinia*. Our findings underscore the critical role of human intervention in preserving habitat suitability, particularly in mitigating the adverse effects of natural succession dominated by shrubs and trees. Furthermore, our approach demonstrates the potential of VHR remote sensing data in mapping small-scale butterfly habitats, offering applicability to habitat mapping for various other species.

Keywords: habitat suitability model (HSM); biotope classification; very high-resolution (VHR) imagery; convolutional neural networks (CNN); marsh fritillary; Hainich National Park



Academic Editor: Dehua Mao

Received: 11 November 2024

Revised: 21 December 2024

Accepted: 3 January 2025

Published: 4 January 2025

Citation: Dietenberger, S.; Mueller, M.M.; Henkel, A.; Dubois, C.; Thiel, C.; Hese, S. Mapping Habitat Structures of Endangered Open Grassland Species (*E. aurinia*) Using a Biotope Classification Based on Very High-Resolution Imagery. *Remote Sens.* **2025**, *17*, 149.

<https://doi.org/10.3390/rs17010149>

Copyright: © 2025 by the authors. Licensee MDPI, Basel, Switzerland. This article is an open access article distributed under the terms and conditions of the Creative Commons Attribution (CC BY) license (<https://creativecommons.org/licenses/by/4.0/>).

1. Introduction

Monitoring ecosystems and implementing effective conservation measures require detailed analysis of habitat conditions and the quantification of habitat structures for endangered species [1]. European open grasslands, known for their high biodiversity, serve as critical habitats for many endangered plant and animal species [2]. Unfortunately, these grasslands have significantly declined or disappeared over recent decades [3,4]. This loss is largely due to the conversion of grasslands into agricultural and urban areas, as well as their transitions into shrubland and forests through natural succession [5–7]. Many butterfly species depend exclusively on grassland ecosystems, with their survival closely tied to specific habitat conditions and plants species, rendering them highly vulnerable to environmental changes [8,9].

The butterfly *Euphydryas aurinia*, commonly known as the marsh fritillary, is distributed across Europe and parts of Asia. However, populations have severely declined in recent decades [10], and the butterfly is listed as an endangered species on the European red list of butterflies [11]. The species is afforded special protection under the EU Habitats Directive, listed in Annex II, requiring EU member states to designate special protection areas [12]. This often regionally monophagous species inhabits flower-rich calcareous grasslands and wet meadows, preferring short, grassy vegetation. Shifts in land use away from open grasslands and eutrophication due to intense fertilization practices have led to its disappearance in several regions. Its dependence on specific habitat conditions, especially the abundance of host plants for the butterfly eggs and larvae, such as *Succisa pratensis* or *Scabiosa columbaria*, has made it particularly vulnerable to habitat changes [13,14]. In Thuringia, Germany, it was once widespread in nutrient-poor wet meadows but now predominantly inhabits dry, scabious-rich grasslands, favoring *Scabiosa columbaria* as its main food source, with *Knautia arvensis* and *Dipsacus fullonum* serving as alternative food plants [15].

Analyzing habitat conditions in terms of the specific environmental factors that influence the presence or absence of *E. aurinia* can provide valuable insights into how to manage open grasslands and conserve this species. These relationships between species' spatial distribution and certain spatial explicit environmental variables (e.g., climate, land cover type, soil, topography) are generally investigated using habitat suitability models (HSM) [16,17]. These models analyze the empirical relationship between species presence and specific habitat conditions by establishing statistical equations, such as Generalized Additive Models (GAMs), Generalized Linear Models (GLMs), Random Forest (RF), Artificial Neural Networks (ANN), or Maximum Entropy (MaxEnt) [18–20]. Defining these relationships provides an understanding of the environmental conditions that promote the occurrence of the species and allows for predicting the probability of species occurrence based on certain habitat conditions, which can then be used to model habitat suitability [18]. In some cases, HSMs are also referred to as species distribution models (SDM), bioclimatic envelope models, or ecological niche models, which are terms used synonymously or with slight differences in their definition and goals. For example, one distinction is whether the model aims to map the potential or the actual distribution of the observed species.

Spatially explicit information on environmental variables needed for HSMs is often derived from remote sensing (RS) data. RS applications can map large study areas that cannot be monitored by in situ surveys. RS has already been used for habitat suitability mapping in a broad range of studies [21], often focusing on a specific animal species such as bird species [22] or termites [23]; plant species such as seagrass [18,24] or Bromeliaceae [25]; and even viruses [26].

The use of RS data and techniques for habitat mapping on different scales depends on the spatial, temporal, and spectral resolution of the available data [1,27–31]. While a

wide range of satellite images with high temporal and spectral resolution is nowadays freely available, the potential of airborne and unmanned aerial vehicle (UAV) data lies in their very high spatial resolution, in the range of a few centimeters. This allows for detailed mapping of landscape-scale habitat structures [27,32–34]. Butterfly species, in particular, often depend on specific micro-habitat structures and have limited mobility. *E. aurinia* is relatively sedentary [35], with most individuals moving less than 100 m between two capturing events [36,37]. This necessitates small-scale monitoring, making VHR data crucial for habitat mapping [38–41].

We analyzed the habitat suitability of *E. aurinia* within the open grassland areas of the Hainich National Park (HNP) in Thuringia, Germany. The analysis integrates an RS land cover type classification with habitat suitability modelling using different HSMs. In the first step, classification based on object-oriented image analysis (OBIA) using VHR airborne RGB data is implemented. In the second step, these classification results are used to model the habitat suitability of the marsh fritillary butterfly. The aim of the habitat analysis is to identify the spatial factors that either favor or hinder the presence of this endangered species in the study site. This knowledge can be used by the HNP administration to improve habitat conditions through targeted management and conservation measures.

Our approach leverages VHR airborne data to facilitate precise mapping of small-scale butterfly habitats. This innovative approach integrates deep learning classification techniques with habitat mapping. Initially tailored for the case study of *E. aurinia*, our method is versatile and can be applied to the small-scale habitat mapping of various other species. As we exclusively utilize an RS-based approach for habitat modeling, our analysis is constrained to a subset of variables delineating land cover characteristics and vegetation structure.

2. Materials

2.1. Study Area: Open Grassland Within Hainich National Park

HNP in the state of Thuringia, central Germany, encompasses a 7,500-ha protected area, primarily managed without any human intervention (Figure 1). It was established in December 1997 on land previously used for military purposes, impeding other human activities. It is part of the special area of conservation “Hainich” and the European network of protected areas “Natura 2000” [42]. The park is situated within a range of hills between 225 and 493 m a.m.s.l. composed of limestone layers (*Muschelkalk*) from the Middle Triassic age [43,44].

While a substantial portion of HNP is characterized by structurally diverse deciduous forests, the southern part comprises an open grassland area interspersed with individual shrubs and trees. The study site is home to several endangered species, including the butterfly *E. aurinia*.

2.2. Data

2.2.1. Remote Sensing Data

Aerial photographs were acquired during two flight campaigns on 22 and 31 July 2020, under sunny weather conditions, utilizing an Ultracam Eagle Mark 3 sensor at an altitude of approximately 3,000 m. The photos were preprocessed to produce RGB and CIR orthomosaic, as well as a Canopy Height Model (CHM). The flight campaign and preprocessing were conducted by the company GeoFly on behalf of the HNP administration. Additionally, a Digital Terrain Model (DTM) from the Thuringian State Office of Land Management and Geological Information (geoportal.thueringen.de) was utilized (Table 1).

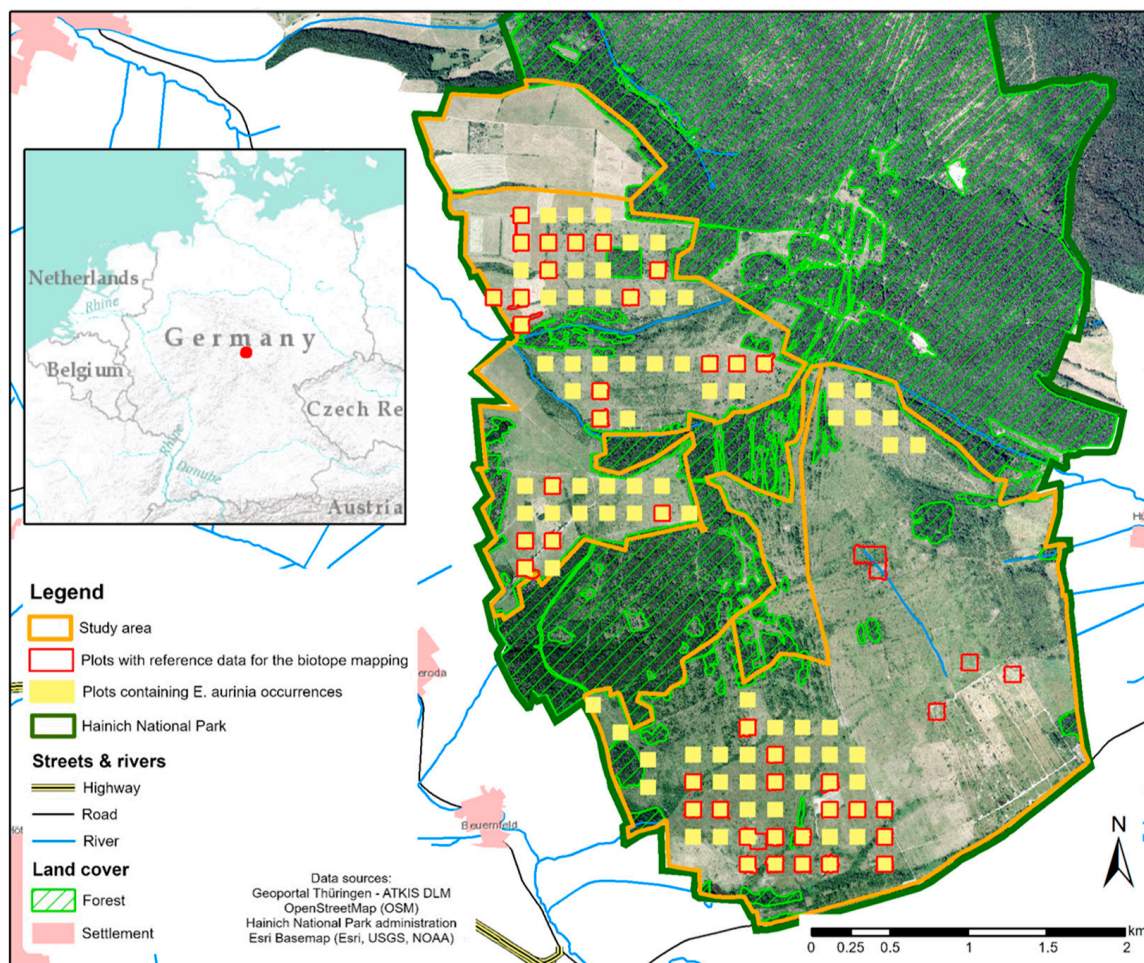


Figure 1. Overview of the study area in the southern part of the HNP in central Germany. Two different types of plots (each 1 ha) have been used for collecting the reference data regarding first the biotope types and second *E. aurinia* occurrences.

Table 1. Overview of the spectral aerial photos and height models used in the analysis. All data use the projected coordinate system ETRS89/UTM Zone 32N (EPSG: 25832).

Dataset	Recording Date	Description	Geometric Resolution
Orthomosaic RGB	July 2020	Spectral bands: R, G, B	0.1 m
Orthomosaic CIR	July 2020	Spectral bands: R, G, NIR	0.1 m
Canopy Height Model (CHM)	July 2020	Height difference between the surface and ground, corresponds to the height of the vegetation	1.0 m
Digital Terrain Model (DTM)	February 2017	Height of the ground surface	0.5 m

2.2.2. Reference Data

This study utilized two reference datasets: one detailing biotope types and the other documenting occurrences of *E. aurinia*. The biotope types were classified using a mapping key based on Arweiler et al. [45]. Both datasets were manually collected in the field by

the Naturforschende Gesellschaft Altenburg (natura2000.nfga.de) on behalf of the HNP administration. The data are organized into 100 x 100 m plots (1 ha each), regularly distributed across the study area (Figure 1). The biotope reference data were georeferenced using a Leica GS004 GNSS (Leica, Wetzlar, Germany) during a field campaign in September and October 2020, covering 47 plots. Each biotope type identified in the field is represented by a polygon. Linear features, such as paths, are converted to polygons by applying a 1 m buffer, resulting in a 2 m width, reflecting the average path width in the study area.

The *E. aurinia* reference dataset includes all recorded butterfly occurrences within 106 plots, represented as point location. Data collection occurred in May 2020, resulting in a total of 2381 documented marsh fritillary occurrences.

3. Methods

The analysis follows two main steps: first, the classification of biotope types using object-based deep learning methods, and second, the application of these classification products in a habitat structure analysis.

3.1. Classification of Biotope Types

The biotope classification employs a hierarchical classification system containing two levels (Figure 2). Segmentation and classification were performed using the software Trimble eCognition (version 9.8).

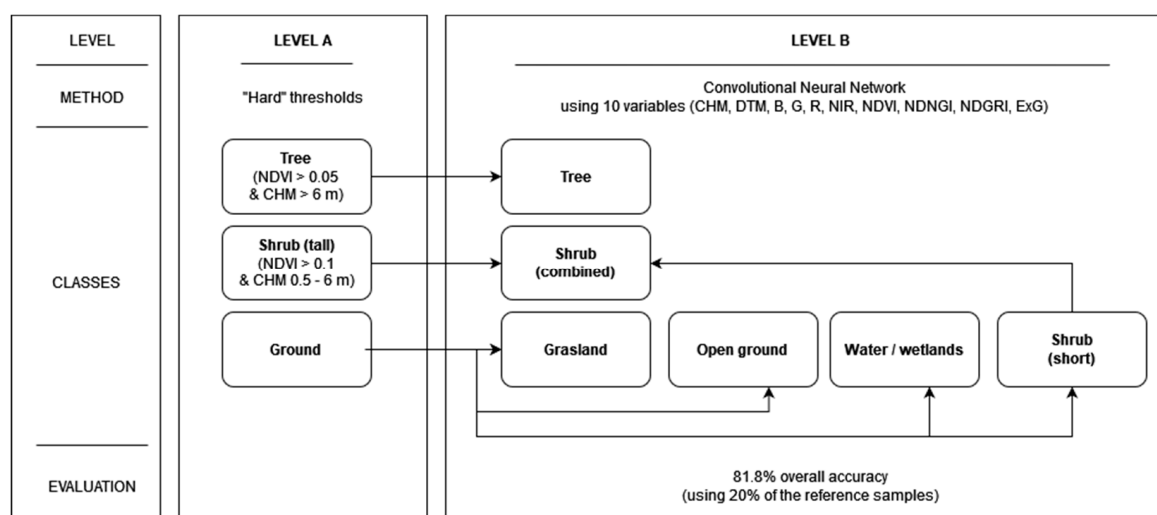


Figure 2. Overview of the methodological system used for the biotope classification.

3.1.1. Segmentation

The biotope mapping is based on an object-oriented classification approach, which requires generating objects prior to classification using a segmentation algorithm:

- Level A: multiresolution segmentation based on CHM with a scale factor of 5
- Level B: multiresolution segmentation based on the spectral bands (B, G, R, NIR) with a scale factor of 100, applied within previously classified "ground" objects

3.1.2. Classification

In addition to thresholding, a deep learning approach using a Convolutional Neural Network (CNN) architecture was employed for classification due to its proven effectiveness in VHR image analysis and object-based classifications [46–49].

Combining spectral and geometric information has been found to be beneficial in various CNN classification tasks [50,51]. Therefore, both spectral and geometric information

were used as inputs, including spectral band layers, height information, and various vegetation indices (Table 2 and Figure 3).

Table 2. Description of the spectral indices used within the separability analysis.

Index	Name	Formula	Source
NDVI	Normalized difference vegetation index	$\frac{NIR-R}{NIR+R}$	[52]
NDGRI	Normalized difference green-red index	$\frac{R-G}{R+G}$	[53]
NDNGI	Normalized difference NIR-green index	$\frac{NIR-G}{NIR+G}$	[54]
ExG	Excess Green Index	$2 \times G - R - B$	[55]

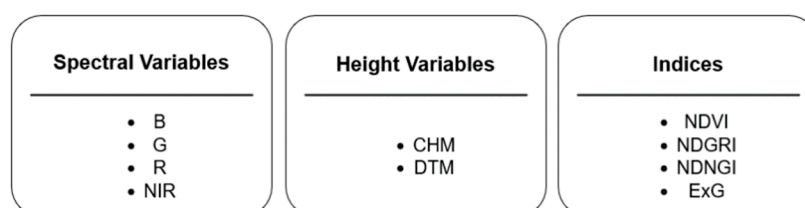


Figure 3. List of variables used as input layers in the CNN model for biotope classification. The indices are explained in Table 2.

The biotope reference dataset was used for training and validation. Due to class size imbalances, a representative sub-selection of samples was manually chosen for larger classes to prevent overestimation of these classes. In total, 20% of the samples were reserved for evaluation and were not used in the training process. Various parameter combinations were tested and refined to improve model accuracy. An overview of the applied parameters is provided in Table 3.

Table 3. Parameter combination applied for the CNN classification of the biotope mapping (level B).

Area	Parameters	Value
Variables	Number of variables	10
Reference data	Samples file format	RAW
	Number of generated samples	20,000
	Size of samples	$32 \times 32 \times 10$
	Division into training:validation	80:20
CNN architecture	Number of intermediate layers	3
	Kernel size 1	3
	Number of feature maps 1	12
	Kernel size 2	4
	Number of feature maps 2	12
	Kernel size 3	3
	Number of feature maps 3	12
Max pooling (1–3)	Yes	
CNN training	Learning rate	0.0006
	Training steps	2000
	Batch size	50
CNN evaluation	Number of samples	1000
	Overall accuracy	81.1%

3.2. Habitat Structure Analysis

3.2.1. Selection and Generation of Variables for the Analysis of the Habitat Structure

A total of 16 variables were selected for analyzing habitat structure and creating the HSM, based on the biotope mapping and RS data (Figure 4).

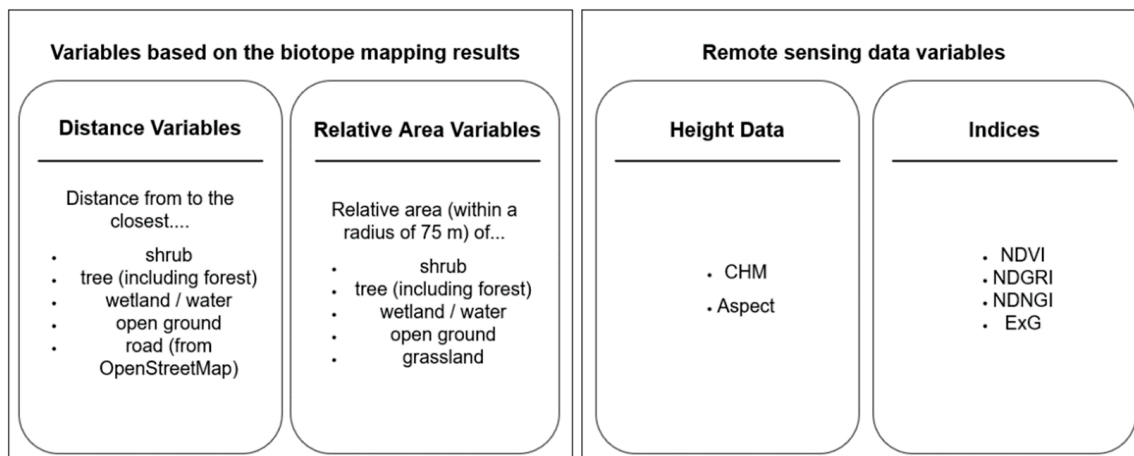


Figure 4. Variables used for the analysis of the habitat structure.

To analyze the impact of certain biotope classes on the habitat of *E. aurinia* and to gain insights into the preferred habitat structure, two types of variables were generated based on the biotope mapping results. The first measures the distance (in meters) to specific biotope classes, while the second quantifies the density or relative area of these classes within a designated radius. These variables were generated separately for shrubs, trees (including forest areas), wetland area, and open ground. Additionally, distance variables for roads were derived from OpenStreetMap (OSM), and relative area variables were calculated for grassland.

For the relative area variables, a threshold must be chosen to represent the species-specific area of influence. Junker and Schmitt [37] suggest that the mobility of most *E. aurinia* individuals does not exceed 60 m, while Junker et al. [36] propose a distance of 100 m. Therefore, a threshold of 75 m was deemed reasonable to calculate the relative area variables. For each pixel, the percentage of the surrounding area occupied by each class was computed, e.g., a value of 0 for the grassland variable indicates no grassland within a radius of 75 m and 1 indicates 100% grassland. All variables were converted to raster data with a pixel size of 1 m and used as input to the HSMs. A comparative analysis using the same data in a higher resolution of 0.25 m did not reveal any relevant deviations in results, but significantly increased computation times.

3.2.2. Modeling the Habitat Suitability of *E. aurinia*

To model the presence and habitat structure of the butterfly, we developed various HSMs using different algorithms such as GLM, GAM, and RF, implemented with the “biomod2” package (version 3.4.6) in R. These algorithms have demonstrated accurate habitat suitability predictions in previous research [56–58]. These models required both presence and absence data; however, our reference data only included presence information. Therefore, we had to generate pseudo-absence (PA) data within the 1 ha plots where presence data were collected (Figure 1).

We employed two methods to generate PA points. The “random pseudo-absence” (R-PA) method involves randomly selecting points within the plots where no butterfly was observed during the field study. However, nearby points to where the butterfly was observed might have similar environmental conditions, which could affect the accuracy of

this method. To address this potential limitation, the “surface range envelope” (SRE-PA) method selects PA points outside the range of variable values observed for the butterfly’s presence. We excluded the lowest and highest 10% of variable values to define this range. This approach aims to select areas where the butterfly is less likely to occur based on the observed environmental conditions [59,60]. Following Barbet-Massin et al. [61], who recommend generating a large number of PA points for models based on regression methods, we generated 5,000 PA points per method. Two separate datasets with the same parameters were created for each method to address the influence of the PA method on model performance.

The RF, GLM, and GAM models were trained with 80% of the data, reserving 20% for validation. We used Overall Accuracy (OA), Cohen’s Kappa Index, and Receiver Operating Characteristics (ROC) to assess the model performance. Models were confined to data within the 1 ha plots, and variable values outside these plots were designated as No-Data. Default parameters were used for the GLM model, while for the GAM model, the “mgcv” package was utilized with the Restricted Maximum Likelihood (REML) method and a smoothing term (k) value of 5. K was chosen through visual elevation of the model output to achieve an optimal fit, balancing under- and overfitting.

Response curves (RCs) were constructed to explore the relationship between variables and butterfly occurrence, based on Elith et al.’s [62] concept of the “evaluation strip”. RCs illustrate the sensitivity of each model to a variable by varying the focal variable across its range while keeping others constant (typically to the mean value). The probability of occurrence of the species is calculated over this range. Interactions between variables were not considered [60,62]. Variable importance was calculated for the RF model.

The GAM and RF models using the SRE-PA dataset had the highest evaluation values and were used to project habitat suitability across the entire study site. Variable values of the entire area were now utilized for this purpose. To reduce the granularity and noise in the prediction map, the resulting GAM model output was filtered using the default gaussian filter from the Orfeo toolbox [63].

To test model transferability to other species, we applied the developed workflow to data of bird breeding territories within the same study area and evaluated the performance.

4. Results

4.1. Results of the Biotope Mapping

Prior to classification, the study site of 18,575 hectares was divided into the two major biotopes of the national park, open grassland and forest, using an existing forest mask. This resulted in 8,611 hectares of forest, which was excluded from the biotope classification. The remaining 9,964 hectares of open grassland were used for classification. Figure 5 displays three subsets of the classification results at level B, achieving an overall accuracy of 81.8%. As expected, grassland represents the largest area, comprising approximately two-thirds (67.95%) of the total area, followed by shrubs (24.66%), open ground (4.51%), trees (2.67%), and wetlands (0.20%).

Shrubs, open ground, trees, and wetlands are not evenly distributed throughout the study area but are concentrated in specific locations. For instance, the presence of shrubs varies across different grassland areas. The middle panel of Figure 5 highlights areas where shrubs are progressively encroaching into open grassland. The gradual transition from grassland to dense shrub and tree cover is visible, representing different stages of bush encroachment. Additionally, certain parts of the study site contain clusters of wetland patches (Figure 5, top panel), which correspond to ponds or depressions that accumulate with water. These wetlands are typically small, with a mean size of 5.1 m² per wetland polygon.

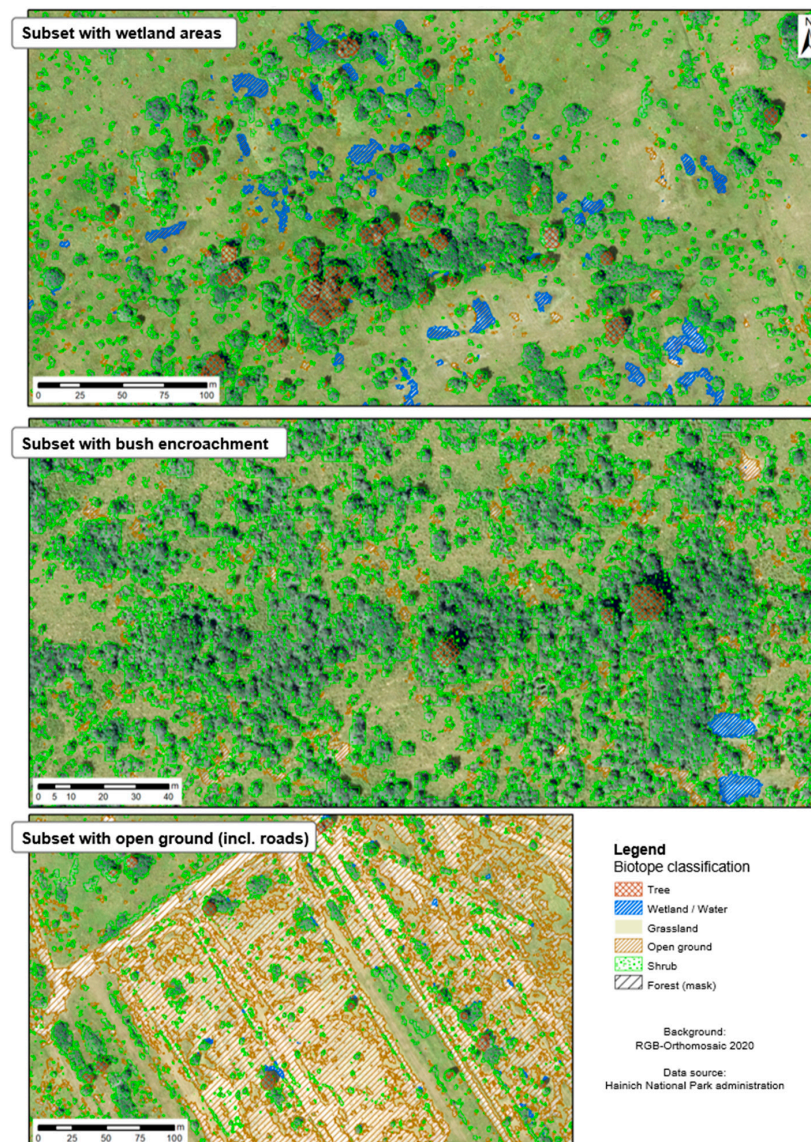


Figure 5. Exemplary subsets of the classification results in biotope types (level B) using a CNN.

4.2. Results of the Habitat Analysis

The results of the habitat analysis are divided into two main areas of focus:

1. Investigating the relationship between different variables and the likelihood of the species' occurrence (Figures 6, 7 and A1)
2. Projecting this probability across the entire study area (Figure 8)

4.2.1. Analysis of the Variable Distribution at the *E. aurinia* Occurrence Sites

Figure 6 shows the distribution of the variable values at the locations where the marsh fritillary was found. Each plot shows the frequency distribution of the respective variable values, providing insights into the habitat conditions that characterize areas occupied by this endangered species.

4.2.2. Results of the HSM

Validation metrics for each model algorithm and the PA dataset are presented in Table 4 for the SRE-PA and R-PA generation method. In general, the differences between the model outputs are within a minor range, with overall accuracy varying between 0.67 and 0.75 across all models and PA generation methods. Among the HSM methods, RF

consistently achieved the highest scores for Kappa, overall accuracy, and ROC, with values up to 0.75. Comparing the two PA generation methods, the SRE-PA method produced slightly better validation metrics for all three models compared to the R-PA method.

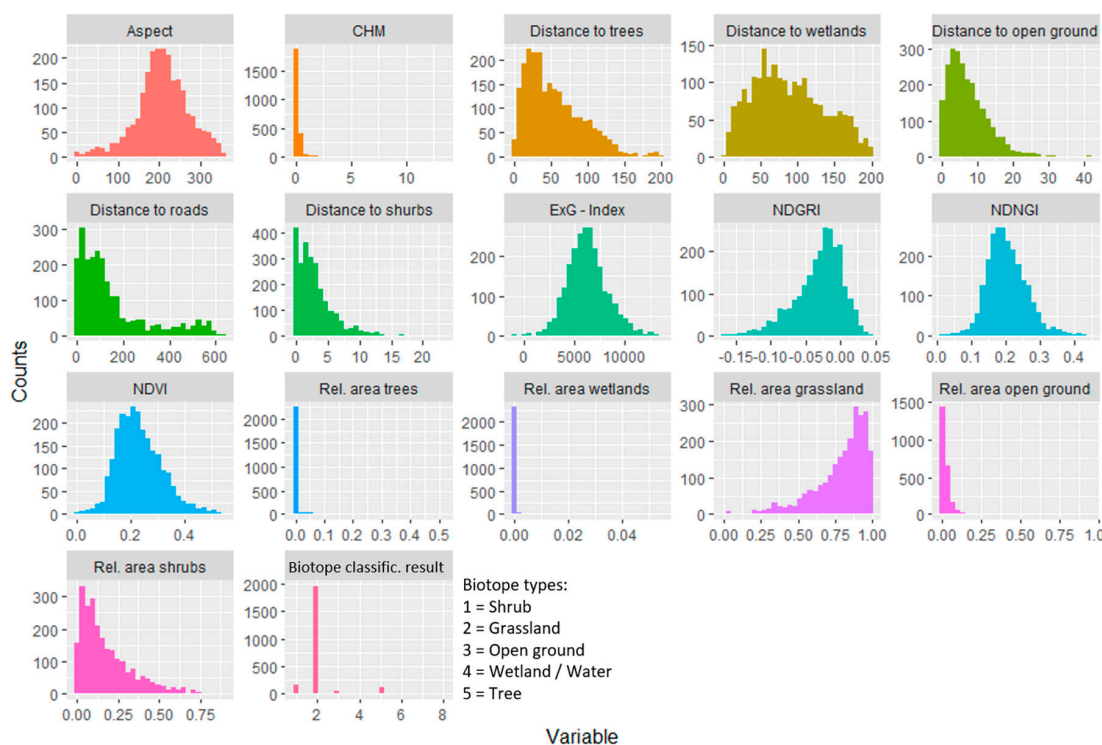


Figure 6. Number of occurrences of *E. aurinia* for the respective variable value.

Table 4. Validation results of the HSM comparing three different methods using pseudo-absence data generated with the SRE-PA method and with a R-PA selection (two datasets for each model).

PA Generation Method	Validation Metrics	GLM, PA Set 1	GLM, PA Set 2	GAM, PA Set 1	GAM, PA Set 2	RF, PA Set 1	RF, PA Set 2
SRE-PA	Kappa-Index	0.25	0.29	0.27	0.29	0.34	0.37
	Overall Accuracy	0.69	0.71	0.70	0.71	0.73	0.75
	ROC	0.69	0.70	0.70	0.71	0.75	0.75
R-PA	Kappa-Index	0.25	0.28	0.26	0.26	0.28	0.31
	Overall Accuracy	0.69	0.69	0.70	0.70	0.71	0.72
	ROC	0.67	0.69	0.69	0.70	0.71	0.72

The transferred model to the data of bird breeding territories achieved similar or even slightly higher accuracy values, with overall accuracy ranging between 0.76 and 0.82, indicating general transferability of the model to other species.

The RCs for the GAM and GLM models using two PA datasets each are depicted in Figure 7 for the SRE-PA method and in Figure A1 for the R-PA method. The RCs of the RF model did not show a discernible trend for any of the variables and datasets and were therefore excluded.

The projection of habitat suitability across the entire study site using the RF and GAM models with the second SRE-PA dataset is illustrated in Figure 8. Lower probability values can be found in both models within homogeneous grassland areas (e.g., in the northwest), along paths and hedges (e.g., in the southwest), and in areas with strong bush encroachment (notably along the eastern border of the study area). Grassland areas with medium presence

of shrubs and trees are declared in both models with medium to high values, although the distribution of these areas, particularly hot spots, differ between the models.

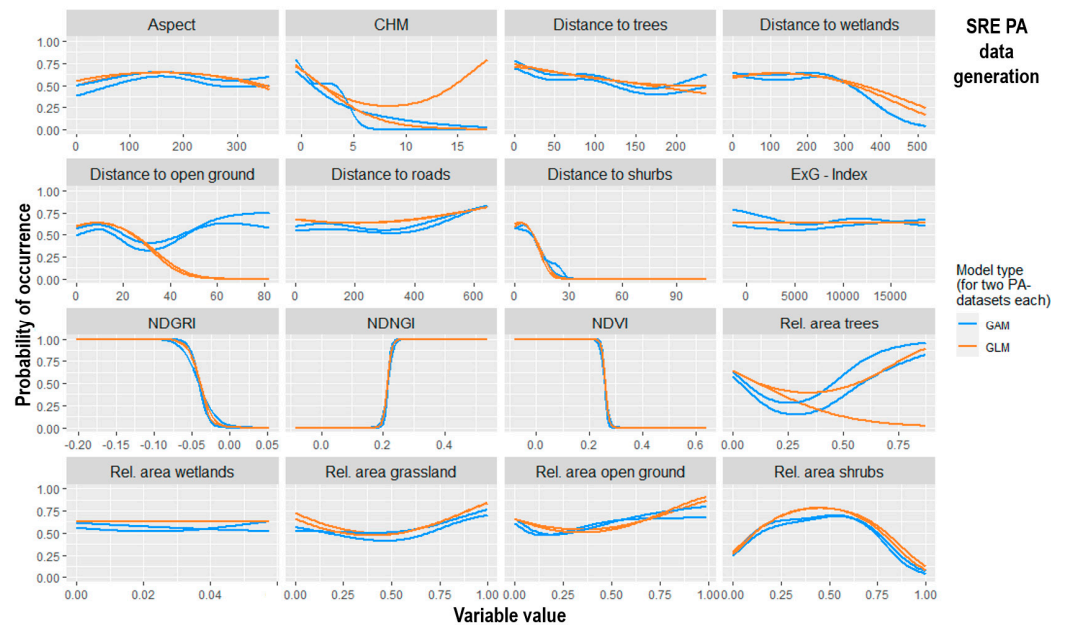


Figure 7. Response curves of the variables used for the GAM and GLM methods to model the marsh fritillary habitat, each for two pseudo-absence datasets generated randomly.

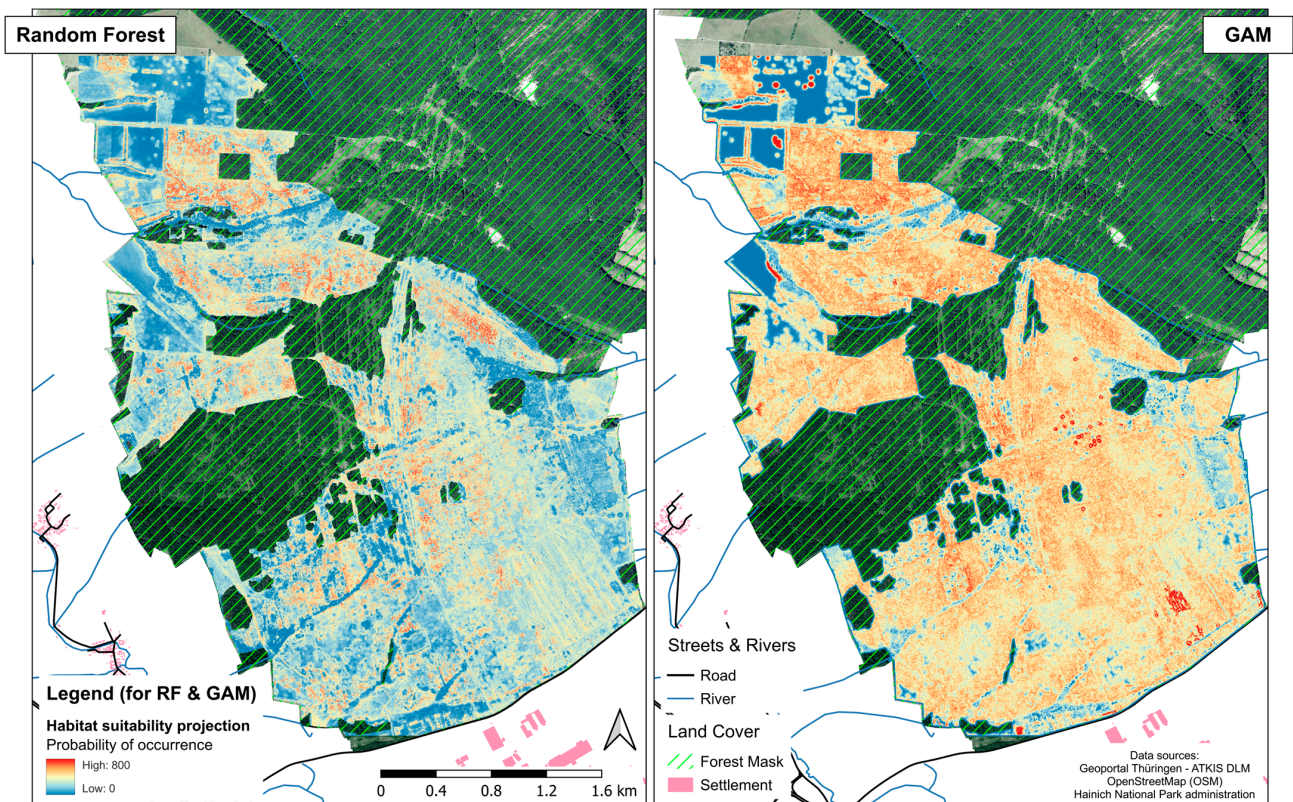


Figure 8. Projection of the habitat suitability for *E. aurinia* across the entire study site utilizing a RF (left) and GAM (right) model, both generated with an SRE-PA dataset. The projections are represented as probability maps, with blue areas indicating low habitat suitability and orange to red areas representing high habitat suitability.

5. Discussion

5.1. Discussion of the Biotope Mapping

The classification at level B using a CNN achieved an 81.8% accuracy rate for correctly assigned samples. One advantage of CNNs is their ability to focus not only on the distribution of variable values but also on the textural features within samples, such as edges [64]. This capability allows for the differentiation of classes even when spectral separability is low.

Visual inspection of the results confirmed successful identification of small shrubs and open ground. Wetlands were accurately delineated in many cases, likely due to differences in NIR values, although misclassification occurred with silted or densely vegetated wetlands. Misclassifications were less prevalent in the sample-based evaluation, as more samples were generated for larger land cover classes, even after manual adjustments to the number of samples per class.

To ensure accurate delineation of path structures, which can be covered with bare soil, stones, or grass, OSM road data were used for habitat modeling. As these data are globally available and in most cases highly detailed, incorporating OSM data can be useful to enhance land cover classification [65,66].

The biotope classification relies on concrete classes, such as tree, shrub, and grassland. However, the study site reveals a natural succession process from grassland to shrubs and ultimately to trees, highlighting the continuous and dynamic nature of ecological phenomena [67,68]. This continuity poses a challenge for categorizing such inherently continuous ecological processes into distinct classes. While our classification approach generally provides clarity, transitional states between grassland and shrubs complicates distinctions. Notably, the presence of grasslands with an herbaceous layer signifies these transitional states, further blurring the boundaries between categories. Moreover, the strict threshold for delineating trees and shrubs (Level A) generally ensures classifications but also risks misclassifying low trees as shrubs. To improve the ecological correctness of biotope classifications, incorporating more distinct classes, such as 'grassland with herbaceous layer', into the mapping process or utilizing continuous classes could be beneficial [69]. However, this approach might introduce additional uncertainties in classification accuracies. Robbins [70] describes this phenomenon as "reversed engineering", where the environment is redesigned to fit technological needs, with land covers adjusted to match planners' concepts [70,71]. Our study emphasizes the importance of acknowledging the dynamic and continuous nature of ecological processes in RS-based biotope classifications, advocating for nuanced approaches to address these complexities.

5.2. Discussion of the Habitat Analysis

This section interprets and evaluates the conducted habitat analysis, beginning with a discussion of the methodology employed and potential sources of uncertainty, followed by an evaluation of the results focused on habitat structure and suitability projections.

5.2.1. Potential Uncertainty Factors in Habitat Modelling and Parameterization

The HSMs employed in this study achieved a moderate overall accuracy of up to 0.75. Bryn et al. [72] systematically analyze potential uncertainty factors and errors throughout the modelling process, emphasizing the importance of selecting the appropriate model, fine-tuning, and setting parameters [72]. Each stage carries different susceptibilities to errors [73]. During the HSM setup, various parameters were scrutinized for their impact on the results, including the choice of the PA method (R-PA, SRE-PA), the choice of a modeling method (GAM, GLM, RF), and the parameter settings of the individual modeling method (e.g., the value k for GAM).

In the marsh fritillary habitat modeling, we examined how two different PA methods affected RCs. The general trend of RCs for both methods aligns across most variables, and the differences between the R-PA and SRE-PA methods are generally narrower than differences observed between the two models or individual runs (Figures A1 and 7). The SRE-PA method slightly outperforms the R-PA method (Table 4), but the difference is marginal, suggesting that in our study, the influence of the PA model is neglectable. This contrasts with several other studies that report a considerable influence of the PA method, especially for regression models [61,74,75].

Overall, the validation resulted in similar accuracies between the model choices (RF, GAM, GLM). However, Fernandes et al. [73] suggest that the models' responses to errors, such as erroneous presence or absence data, could differ. RF may overfit by incorporating errors while maintain higher accuracy values, whereas GLM can effectively mitigate errors in the training data [73]. This might explain why, despite slightly higher accuracy values in the RF model, it was unable to produce a trend in the RC [73]. On the other hand, the RCs between the two regression methods, GAM and GLM, generally exhibit similar trends across most variables. However, some curves show some degree of random variability across multiple runs with the same parameter settings. This variability was higher for certain variables, such as the vegetation indices used (Table 2), while distance variables demonstrated lower random variability. The RCs for the indices displayed partially opposing trends between different runs with the same settings, whereas distance variables were more robust to both random variability and varying parameters.

Regarding the choice of suitable parameters, the smoothing term k is particularly important, as it alters the degree to which the model is fitted to the data, exerting a relatively large influence on the RCs.

5.2.2. Analysis of Habitat Variables on Species Presence

The distribution of *E. aurinia* occurrences for specific variable values (Figure 6) indicates a normal distribution for most variables. The butterflies tend to be found near bushes, trees, and roads, except for the distance to wetlands, which does not exhibit a clear pattern. Grassland predominates around the occurrence points, as expected. Many points are located on south-facing surfaces, which may partially reflect the overall distribution of pixel values in the study area, primarily south-facing, and may not explicitly represent habitat suitability. Here, the RCs of the HSMs offer a decisive advantage by contrasting presence data with PA data.

The RCs for variables related to the biotope class "shrubs" are particularly consistent across different runs (Figure A1 and Figure 7) and exhibit high variable importance in the RF model (Figure A2). Two notable trends emerged:

1. Proximity to shrubs: higher habitat suitability is observed near shrubs, with the probability of occurrence decreasing to 0 at approximately 30 m from the nearest bush.
2. Shrub encroachment: excessive bush encroachment negatively impacts habitat suitability, as reflected by the variable "relative area shrubs". Both very low and very high proportions of shrubs in the vicinity reduce the likelihood of finding the butterfly. This aligns with the well-established fact that the marsh fritillary disappears as succession progresses and open grassland becomes dominated by shrubs and trees [10,76]. This underscores the necessity for human management to counteract natural succession and preserve habitat suitability, as emphasized in prior studies [77]. Interestingly, our findings suggest that the species also benefits from the vicinity of shrubs, with an optimal state observed at around 25-60% relative area of shrubs.

In contrast, an opposite trend is observed for tree density, with the probability of *E. aurinia* occurrence consistently decreasing as tree density increases, particularly between

0–25% relative area of trees. For higher tree densities, the trend becomes less clear. This decrease in probability may be attributed to *E. aurinia*'s aversion to shady areas and its preference for easily accessible, sun-exposed host plants for larval development [14,78].

Our findings also suggest that *E. aurinia* occupies moist meadows, as indicated by a modest reduction in butterfly presence likelihood with increased distance from the nearest wetland area, notably beyond approximately 300 m. This complements rather than contradicts the species' association with dry grassland habitats in Thuringia [15], acknowledging that the species is also known to inhabit moist meadows [9,36].

5.2.3. Projections and Spatial Patterns of Habitat Suitability

When evaluating the projections of the HSM, it is important to recognize that these models identify sites with high or low habitat suitability based solely on the variables employed. Other potentially unknown influencing factors are not included in the projection.

While the overall distribution of cold spots, representing areas with low habitat suitability, is largely consistent between the RF and GAM, notable differences emerge in the identification of hot spots.

Both models agree that areas dominated by homogeneous grassland without shrubs or trees and those with dense bush encroachment are unsuitable habitats. Also, linear paths and hedge structures exhibit lower probability values in both models. This aligns with findings from Betzholtz et al. [78] and Botham et al. [35], who emphasize the significance of vegetation height in influencing the butterfly's occurrence, with optimal heights ranging from 4 to 16 cm [78], a condition which may not be met in either homogeneous grasslands or dense shrub areas. The importance of vegetation height in general is also reflected in the high variable importance value of the CHM in the RF model (Figure A2).

However, the models diverge in their predictions of high-suitability areas. GAM particularly identifies hot spots near wetland patches, as visible in the southeast and the center of the study area. The model interprets wetlands and their immediate surroundings (up to a 10 m distance) as important environmental factors for high habitat suitability, reflecting the role these areas play in the butterfly's presence [9,36]. This was similarly found in the RC of the GAM and GLM models, as discussed in the previous section. In contrast, the RF model does not assign any importance in the presence of wetlands. This fact is also reflected in the minor importance of the two wetland variables in the RF variable importance (Figure A2).

RF predicts hot spot areas primarily in areas characterized by medium levels of bush and tree encroachment, particularly scattered across the northern part of the study site. These areas are also categorized as having medium to high suitability in the GAM model. Both models agree on the general habitat suitability of areas featuring a patchy mosaic of grasslands interspersed with individual shrubs and trees, which may provide a more diverse structural habitat. However, RF tends to identify specific locations, compared to more general hot spot areas identified by GAM.

These differences might be attributed to the different underlying model architectures. As an ensemble machine learning method, RF can capture complex, non-linear relationships between predictor variables and habitat suitability, and may identify subtle spatial patterns or combinations of variables that influence habitat suitability, leading to more fragmented or localized predictions of hotspots. By contrast, GAM uses smooth functions to model relationships between predictors and the response variable. While GAMs allow for non-linear effects, their smooth nature can result in more generalized predictions [79]. This smoothing can reduce sensitivity to fine-scale spatial variability, potentially leading to broader and more continuous hot spot areas compared to RF. Additionally, both models can incorporate noise into their predictions through overfitting [73,80].

In general, both habitat projections reveal distinct landscape structures reflected in high or low habitat gradients (Figure 8). This phenomenon is notably pronounced in the RF models' projections, but it is also observable in the GAM model. The differences highlight the unique ways each model interprets the data and prioritize specific environmental predictors. Similar findings have been reported in several other studies, which observed variations in prediction maps across modeling techniques [80–82]. For instance, Kosicki [81] compared RF and GAM and concluded, consistent with our results, that the models differ notably in their approach to assessing the importance of predicting variables and the ecological complexity of the target species.

These findings emphasize the importance of accounting for differences in model architecture when interpreting habitat suitability predictions. Relying on a single model may lead to an incomplete understanding of habitat suitability, especially for complex species-environment relationships. While both RF and GAM produce plausible results, their focus on different aspects of the habitat underscores the value of a multi-model approach. This recommendation aligns with other studies, which advocate for using ensemble modeling approaches to improve predictive accuracy [82–84].

6. Conclusions

This study provided a comprehensive analysis of habitat suitability for the marsh fritillary (*E. aurinia*) within the HNP in Thuringia, Germany, offering valuable insights into the spatial factors influencing the occurrence of this endangered species. We demonstrated that combining VHR RS images with deep learning classification techniques can produce fine-scale spatial variables to model habitat suitability. For instance, distance and density variables were created to analyze biotope types affecting the butterfly's presence. Among other findings, we discussed the role of shrubs in habitat suitability, revealing higher habitat suitability near shrubs and a negative impact of excessive bush encroachment.

By using CNNs for biotope mapping, we contribute to a growing body of studies that successfully implement similar approaches [85–87]. Our finding suggests that combining spectral and geometric data in VHR images, along with enhancing deep learning techniques with rule-based methods, can improve classification results. Additionally, we advocate for the use of continuous variables to overcome the limitations of categorizing non-discrete ecological phenomena.

Employing various modeling techniques such as GLM, GAM, and RF, we scrutinized the influence of different modeling parameters and PA methods on model performance. While the PA method has only a minor influence on our output, the choice of model type notably impacts RC and predictions.

In the habitat suitability modeling, both RF and GAM provided plausible predictions, with moderate accuracy (up to 0.75), and aligned on unsuitable habitats such as homogeneous grasslands, dense bush encroachment, and linear structures. However, the models differed in their identification of high-suitability areas, reflecting their unique interpretations of environmental variables, such as the influence of wetlands.

In conclusion, the applied method offers practical insights for habitat management strategies in conservation areas. Our findings underscore the critical role of human management intervention in preserving habitat suitability, particularly in mitigating the adverse effects of natural succession dominated by shrubs and trees.

Author Contributions: Conceptualization, S.H., A.H. and S.D.; Methodology, S.D., S.H. and A.H.; Software, S.D.; Validation, S.D., A.H. and S.H.; Formal Analysis, S.D., M.M.M., S.H. and C.T.; Investigation, S.D., S.H., A.H. and C.D.; Resources, S.H., C.T., C.D. and A.H.; Data Curation, S.D., M.M.M., S.H. and A.H.; Writing—Original Draft Preparation, S.D. and M.M.M.; Writing—Review and Editing, S.D., M.M.M., C.D., S.H., A.H. and C.T.; Visualization, S.D.; Supervision, S.H., C.D. and

C.T.; Project Administration, S.H.; Funding Acquisition, S.H. All authors have read and agreed to the published version of the manuscript.

Funding: This research received no external funding.

Data Availability Statement: The data presented in this study are available on request from the corresponding author. The data are not publicly available due to privacy reasons.

Acknowledgments: We thank the Hainich National Park administration for their cooperation and their valuable contribution in data collection and sharing. We also gratefully acknowledge the Naturforschende Gesellschaft Altenburg for their support in data collection.

Conflicts of Interest: The authors declare no conflicts of interest.

Appendix A

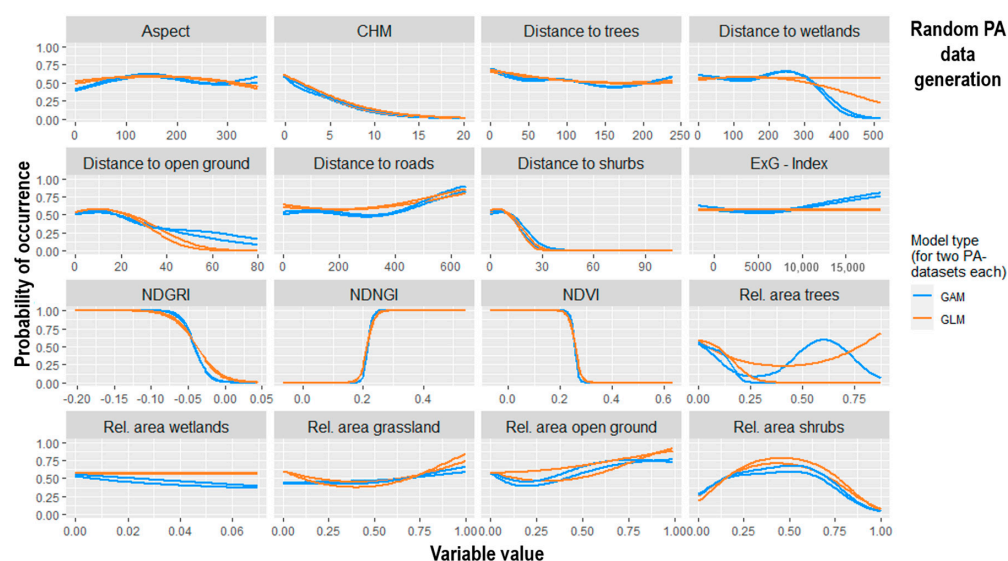


Figure A1. Response curves of the variables used for the GAM and GLM methods to model the marsh fritillary habitat, each for two PA datasets generated with the SRE-PA method.

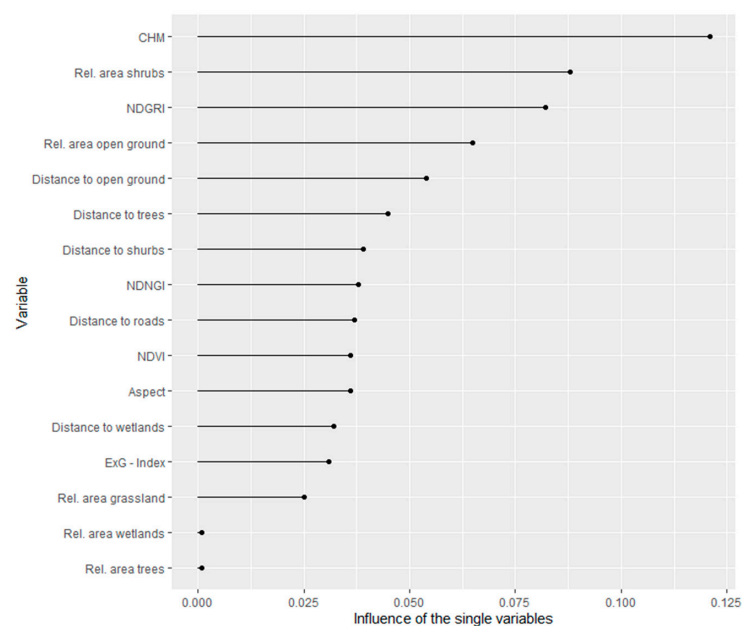


Figure A2. Variable importance in the RF model. Higher values indicate a greater influence of the variable on the model output. The variable importance was calculated using the HSM with the SRE-PA dataset 2.

References

- Alvarez-Vanhard, E.; Houet, T.; Mony, C.; Lecoq, L.; Corpetti, T. Can UAVs fill the gap between in situ surveys and satellites for habitat mapping? *Remote Sens. Environ.* **2020**, *243*, 111780. [[CrossRef](#)]
- Hochkirch, A.; Bilz, M.; Ferreira, C.C.; Danielczak, A.; Allen, D.; Nieto, A.; Rondinini, C.; Harding, K.; Hilton-Taylor, C.; Pollock, C.M.; et al. A multi-taxon analysis of European Red Lists reveals major threats to biodiversity. *PLoS ONE* **2023**, *18*, e0293083. [[CrossRef](#)] [[PubMed](#)]
- Schils, R.L.; Bufo, C.; Rhymer, C.M.; Francksen, R.M.; Klaus, V.H.; Abdalla, M.; Milazzo, F.; Lellei-Kovács, E.; Berge, H.t.; Bertora, C.; et al. Permanent grasslands in Europe: Land use change and intensification decrease their multifunctionality. *Agric. Ecosyst. Environ.* **2022**, *330*, 107891. [[CrossRef](#)]
- Prangel, E.; Kasari-Toussaint, L.; Neuenkamp, L.; Noreika, N.; Karise, R.; Marja, R.; Ingerpuu, N.; Kupper, T.; Keerberg, L.; Oja, E.; et al. Afforestation and abandonment of semi-natural grasslands lead to biodiversity loss and a decline in ecosystem services and functions. *J. Appl. Ecol.* **2023**, *60*, 825–836. [[CrossRef](#)]
- Habel, J.C.; Dengler, J.; Janišová, M.; Török, P.; Wellstein, C.; Wiezik, M. European grassland ecosystems: Threatened hotspots of biodiversity. *Biodivers Conserv.* **2013**, *22*, 2131–2138. [[CrossRef](#)]
- Feurdean, A.; Ruprecht, E.; Molnár, Z.; Hutchinson, S.M.; Hickler, T. Biodiversity-rich European grasslands: Ancient, forgotten ecosystems. *Biol. Conserv.* **2018**, *228*, 224–232. [[CrossRef](#)]
- Schüle, M.; Heinken, T.; Fartmann, T. Long-term effects of environmental alterations in protected grasslands—Land-use history determines changes in plant species composition. *Ecol. Eng.* **2023**, *188*, 106878. [[CrossRef](#)]
- García-Barros, E.; Fartmann, T. Butterfly oviposition: Sites, behaviour and modes. In *Ecology of Butterflies in Europe*; Cambridge University Press: Cambridge, MA, USA, 2009; pp. 29–42. ISBN 978-0-521-74759-2.
- Schlegel, J.; Hofstetter, A. Butterflies of fragmented wet grassland in Western European lowland forests: Effects of vegetation, connectivity and plot size. *Acta Oecologica* **2021**, *110*, 103691. [[CrossRef](#)]
- Schtickzelle, N.; Choutt, J.; Goffart, P.; Fichet, V.; Baguette, M. Metapopulation dynamics and conservation of the marsh fritillary butterfly: Population viability analysis and management options for a critically endangered species in Western Europe. *Biol. Conserv.* **2005**, *126*, 569–581. [[CrossRef](#)]
- van Swaay, C.; Cuttelod, A.; Collins, S.; Maes, D.; López Munguira, M.; Šašić, M.; Settele, J.; Verovnik, R.; Verstrael, T.; Warren, M.; et al. *European Red List of Butterflies*; Publications Office of the European Union: Luxembourg, 2010; ISBN 9789279141515.
- Council Directive 92/43/EEC of 21 May 1992 on the Conservation of Natural Habitats and of Wild Fauna and Flora. *Off. J. Eur. Communities L 206* **1992**, 0007–0050.
- Brunbjerg, A.K.; Høye, T.T.; Eskildsen, A.; Nygaard, B.; Damgaard, C.F.; Ejrnæs, R. The collapse of marsh fritillary (*Euphydryas aurinia*) populations associated with declining host plant abundance. *Biol. Conserv.* **2017**, *211*, 117–124. [[CrossRef](#)]
- Anthes, N.; Fartmann, T.; Hermann, G.; Kaule, G. Combining larval habitat quality and metapopulation structure—The key for successful management of pre-alpine *Euphydryas aurinia* colonies. *J. Insect Conserv.* **2003**, *7*, 175–185. [[CrossRef](#)]
- Verwaltung Nationalpark Hainich, *Managementplan (Fachbeitrag Offenland) für das FFH-Gebiet 036 und SPA-Gebiet 14 "Hainich" (DE 4828-301)—Abschlussbericht: Südliche Teilfläche (Nationalpark Hainich + Umfeld im Wartburgkreis)*; Verwaltung Nationalpark Hainich: Bad Langensalza, Germany, 2018.
- Bradley, B.A.; Olsson, A.D.; Wang, O.; Dickson, B.G.; Pelech, L.; Sesnie, S.E.; Zachmann, L.J. Species detection vs. habitat suitability: Are we biasing habitat suitability models with remotely sensed data? *Ecol. Model.* **2012**, *244*, 57–64. [[CrossRef](#)]
- Guisan, A.; Zimmermann, N.E. Predictive habitat distribution models in ecology. *Ecol. Model.* **2000**, *135*, 147–186. [[CrossRef](#)]
- Bertelli, C.M.; Stokes, H.J.; Bull, J.C.; Unsworth, R.K.F. The use of habitat suitability modelling for seagrass: A review. *Front. Mar. Sci.* **2022**, *9*, 74–81. [[CrossRef](#)]
- Roy, S.; Suman, A.; Ray, S.; Saikia, S.K. Use of species distribution models to study habitat suitability for sustainable management and conservation in the Indian subcontinent: A decade's retrospective. *Front. Sustain. Resour. Manag.* **2022**, *1*, 1031646. [[CrossRef](#)]
- Piri Sahragard, H.; Ajourlo, M.; Karami, P. Landscape structure and suitable habitat analysis for effective restoration planning in semi-arid mountain forests. *Ecol. Process.* **2021**, *10*, 17. [[CrossRef](#)]
- Corbane, C.; Lang, S.; Pipkins, K.; Alleaume, S.; Deshayes, M.; García Millán, V.E.; Strasser, T.; Vanden Borre, J.; Toon, S.; Michael, F. Remote sensing for mapping natural habitats and their conservation status—New opportunities and challenges. *Int. J. Appl. Earth Obs. Geoinf.* **2015**, *37*, 7–16. [[CrossRef](#)]
- Ikhumhen, H.O.; Li, T.; Lu, S.; Matomela, N. Assessment of a novel data driven habitat suitability ranking approach for *Larus relictus* specie using remote sensing and GIS. *Ecol. Model.* **2020**, *432*, 109221. [[CrossRef](#)]
- Ozsahin, E.; Ozdes, M.; Smith, A.C.; Yang, D. Remote Sensing and GIS-Based Suitability Mapping of Termite Habitat in the African Savanna: A Case Study of the Lowveld in Kruger National Park. *Land* **2022**, *11*, 803. [[CrossRef](#)]
- Bakirman, T.; Gumusay, M.U. A novel GIS-MCDA-based spatial habitat suitability model for *Posidonia oceanica* in the Mediterranean. *Environ. Monit. Assess.* **2020**, *192*, 231. [[CrossRef](#)]

25. Judith, C.; Schneider, J.V.; Schmidt, M.; Ortega, R.; Gaviria, J.; Zizka, G. Using high-resolution remote sensing data for habitat suitability models of Bromeliaceae in the city of Mérida, Venezuela. *Landscape Urban Plan.* **2013**, *120*, 107–118. [[CrossRef](#)]
26. Machado-Machado, E.A. Empirical mapping of suitability to dengue fever in Mexico using species distribution modeling. *Appl. Geogr.* **2012**, *33*, 82–93. [[CrossRef](#)]
27. Woellner, R.; Wagner, T.C. Saving species, time and money: Application of unmanned aerial vehicles (UAVs) for monitoring of an endangered alpine river specialist in a small nature reserve. *Biol. Conserv.* **2019**, *233*, 162–175. [[CrossRef](#)]
28. Adamo, M.; Tomaselli, V.; Tarantino, C.; Vicario, S.; Veronico, G.; Lucas, R.; Blonda, P. Knowledge-Based Classification of Grassland Ecosystem Based on Multi-Temporal WorldView-2 Data and FAO-LCCS Taxonomy. *Remote Sens.* **2020**, *12*, 1447. [[CrossRef](#)]
29. Amani, M.; Foroughnia, F.; Moghimi, A.; Mahdavi, S.; Jin, S. Three-Dimensional Mapping of Habitats Using Remote-Sensing Data and Machine-Learning Algorithms. *Remote Sens.* **2023**, *15*, 4135. [[CrossRef](#)]
30. Baena, S.; Boyd, D.S.; Moat, J. UAVs in pursuit of plant conservation—Real world experiences. *Ecol. Inform.* **2018**, *47*, 2–9. [[CrossRef](#)]
31. Kwong, I.H.Y.; Wong, F.K.K.; Fung, T.; Liu, E.K.Y.; Lee, R.H.; Ng, T.P.T. A Multi-Stage Approach Combining Very High-Resolution Satellite Image, GIS Database and Post-Classification Modification Rules for Habitat Mapping in Hong Kong. *Remote Sens.* **2022**, *14*, 67. [[CrossRef](#)]
32. Cruz, C.; O’Connell, J.; McGuinness, K.; Martin, J.R.; Perrin, P.M.; Connolly, J. Assessing the effectiveness of UAV data for accurate coastal dune habitat mapping. *Eur. J. Remote Sens.* **2023**, *56*, 2191870. [[CrossRef](#)]
33. Hodgson, J.C.; Baylis, S.M.; Mott, R.; Herrod, A.; Clarke, R.H. Precision wildlife monitoring using unmanned aerial vehicles. *Sci. Rep.* **2016**, *6*, 22574. [[CrossRef](#)] [[PubMed](#)]
34. Lu, B.; He, Y. Species classification using Unmanned Aerial Vehicle (UAV)-acquired high spatial resolution imagery in a heterogeneous grassland. *ISPRS J. Photogramm. Remote Sens.* **2017**, *128*, 73–85. [[CrossRef](#)]
35. Botham, M.S.; Ash, D.; Aspey, N.; Bourn, N.A.D.; Bulman, C.R.; Roy, D.B.; Swain, J.; Zannese, A.; Pywell, R.F. The effects of habitat fragmentation on niche requirements of the marsh fritillary, *Euphydryas aurinia*, (Rottensburg, 1775) on calcareous grasslands in southern UK. *J. Insect Conserv.* **2011**, *15*, 269–277. [[CrossRef](#)]
36. Junker, M.; Rákósy, L.; Schmitt, T. Moderate mobility and high density in a small area: The population ecology of the marsh fritillary *Euphydryas aurinia* in Transylvania (Romania). *Biol. Futur.* **2023**, *74*, 457–465. [[CrossRef](#)]
37. Junker, M.; Schmitt, T. Demography, dispersal and movement pattern of *Euphydryas aurinia* (Lepidoptera: Nymphalidae) at the Iberian Peninsula: An alarming example in an increasingly fragmented landscape? *J. Insect Conserv.* **2010**, *14*, 237–246. [[CrossRef](#)]
38. Habel, J.C.; Teucher, M.; Ulrich, W.; Bauer, M.; Rödder, D. Drones for butterfly conservation: Larval habitat assessment with an unmanned aerial vehicle. *Landscape Ecol.* **2016**, *31*, 2385–2395. [[CrossRef](#)]
39. Krämer, B.; Kämpf, I.; Enderle, J.; Poniatowski, D.; Fartmann, T. Microhabitat selection in a grassland butterfly: A trade-off between microclimate and food availability. *J. Insect Conserv.* **2012**, *16*, 857–865. [[CrossRef](#)]
40. Davis, M.L.; Barker, C.; Powell, I.; Porter, K.; Ashton, P. Combining modelling, field data and genetic variation to understand the post-reintroduction population genetics of the Marsh Fritillary butterfly (*Euphydryas aurinia*). *J. Insect Conserv.* **2021**, *25*, 875–886. [[CrossRef](#)]
41. Ivosevic, B.; Han, Y.-G.; Kwon, O. Monitoring butterflies with an unmanned aerial vehicle: Current possibilities and future potentials. *J. Ecol. Environ.* **2017**, *41*, 12. [[CrossRef](#)]
42. Bundesamt für Naturschutz. Natura 2000 Gebiete in Deutschland: Hainich. Available online: <https://www.bfn.de/natura-2000-gebiet/hainich> (accessed on 23 July 2024).
43. Schramm, H. Exkursionsführer zur Tagung der AG Forstliche Standorts- und Vegetationskunde vom 18. bis 21. Mai 2005 in Thüringen. In *Naturräumliche Gliederung der Exkursionsgebiete*; Thüringer Landesamt für Wald, Jagd und Fischerei: Gotha, Germany, 2005; pp. 8–19.
44. *Thüringer Gesetz über den Nationalpark Hainich*; ThürNPHG: Freistaat Thüringen, Germany, 1997.
45. *Systematik der Biotoptypen- und Nutzungstypenkartierung (Kartieranleitung): Standard-Biotoptypen und Nutzungstypen für die CIR-Luftbild-gestützte Biotoptypen- und Nutzungstypenkartierung für die Bundesrepublik Deutschland*; Arweiler, F., Bürger, A., Dingler, B., Eds.; Bundesamt für Naturschutz: Bonn, Germany, 2002; ISBN 978-3-7843-3611-4.
46. Kattenborn, T.; Eichel, J.; Fassnacht, F.E. Convolutional Neural Networks enable efficient, accurate and fine-grained segmentation of plant species and communities from high-resolution UAV imagery. *Sci. Rep.* **2019**, *9*, 17656. [[CrossRef](#)]
47. Kattenborn, T.; Leitloff, J.; Schiefer, F.; Hinz, S. Review on Convolutional Neural Networks (CNN) in vegetation remote sensing. *ISPRS J. Photogramm. Remote Sens.* **2021**, *173*, 24–49. [[CrossRef](#)]
48. Zang, N.; Cao, Y.; Wang, Y.; Huang, B.; Zhang, L.; Mathiopoulos, P.T. Land-Use Mapping for High-Spatial Resolution Remote Sensing Image Via Deep Learning: A Review. *IEEE J. Sel. Top. Appl. Earth Obs. Remote Sens.* **2021**, *14*, 5372–5391. [[CrossRef](#)]

49. Mäyrä, J.; Keski-Saari, S.; Kivinen, S.; Tanhuanpää, T.; Hurskainen, P.; Kullberg, P.; Poikolainen, L.; Viinikka, A.; Tuominen, S.; Kumpula, T.; et al. Tree species classification from airborne hyperspectral and LiDAR data using 3D convolutional neural networks. *Remote Sens. Environ.* **2021**, *256*, 112322. [[CrossRef](#)]
50. Polonen, I.; Annala, L.; Rahkonen, S.; Nevalainen, O.; Honkavaara, E.; Tuominen, S.; Viljanen, N.; Hakala, T. Tree Species Identification Using 3D Spectral Data and 3D Convolutional Neural Network. In Proceedings of the 2018 9th Workshop on Hyperspectral Image and Signal Processing: Evolution in Remote Sensing (WHISPERS), Amsterdam, The Netherlands, 23–26 September 2018; IEEE: Piscataway, NJ, USA, 2018; pp. 1–5, ISBN 978-1-7281-1581-8.
51. Zhou, K.; Ming, D.; Lv, X.; Fang, J.; Wang, M. CNN-based Land Cover Classification Combining Stratified Segmentation and Fusion of Point Cloud and Very High-Spatial Resolution Remote Sensing Image Data. *Remote Sens.* **2019**, *11*, 2065. [[CrossRef](#)]
52. Rouse, J.W., Jr.; Haas, R.H.; Schell, J.A.; Deering, D.W. *Monitoring Vegetation Systems in the Great Plains with ERTS*; Goddard Space Flight Center 3d ERTS-1 Symp., Vol. 1, Sect. A; NASA: Washington, DC, USA, 1974; p. 309.
53. Tucker, C.J. Red and photographic infrared linear combinations for monitoring vegetation. *Remote Sens. Environ.* **1979**, *8*, 127–150. [[CrossRef](#)]
54. Moges, S.M.; Raun, W.R.; Mullen, R.W.; Freeman, K.W.; Johnson, G.V.; Solie, J.B. Evaluation of Green, Red, and Near Infrared Bands for Predicting Winter Wheat Biomass, Nitrogen Uptake, and Final Grain Yield. *J. Plant Nutr.* **2005**, *27*, 1431–1441. [[CrossRef](#)]
55. Yang, W.; Wang, S.; Zhao, X.; Zhang, J.; Feng, J. Greenness identification based on HSV decision tree. *Inf. Process. Agric.* **2015**, *2*, 149–160. [[CrossRef](#)]
56. Bektas, V.; Bettinger, P.; Nibbelink, N.; Siry, J.; Merry, K.; Henn, K.A.; Stober, J. Habitat Suitability Modeling of Rare Turkeybeard (*Xerophyllum asphodeloides*) Species in the Talladega National Forest, Alabama, USA. *Forests* **2022**, *13*, 490. [[CrossRef](#)]
57. Jung, J.B.; Park, G.E.; Kim, H.J.; Huh, J.H.; Um, Y. Predicting the Habitat Suitability for *Angelica gigas* Medicinal Herb Using an Ensemble Species Distribution Model. *Forests* **2023**, *14*, 592. [[CrossRef](#)]
58. Rowden, A.A.; Anderson, O.F.; Georgian, S.E.; Bowden, D.A.; Clark, M.R.; Pallentin, A.; Miller, A. High-Resolution Habitat Suitability Models for the Conservation and Management of Vulnerable Marine Ecosystems on the Louisville Seamount Chain, South Pacific Ocean. *Front. Mar. Sci.* **2017**, *4*, 335. [[CrossRef](#)]
59. Busby, J.R. BIOCLIM—A bioclimate analysis and prediction system. In *Nature Conservation: Cost Effective Biological Surveys and Data Analysis*; Margules, C.R., Austin, M.P., Eds.; CSIRO: Canberra, Australia, 1991; pp. 64–68, ISBN 0643050892.
60. Thuiller, W.; Lafourcade, B.; Araujo, M. BIOMOD—A platform for ensemble forecasting of species distributions. *Ecography* **2009**, *32*, 369–373. [[CrossRef](#)]
61. Barbet-Massin, M.; Jiguet, F.; Albert, C.H.; Thuiller, W. Selecting pseudo-absences for species distribution models: How, where and how many? *Methods Ecol Evol* **2012**, *3*, 327–338. [[CrossRef](#)]
62. Elith, J.; Ferrier, S.; Huettmann, F.; Leathwick, J. The evaluation strip: A new and robust method for plotting predicted responses from species distribution models. *Ecol. Model.* **2005**, *186*, 280–289. [[CrossRef](#)]
63. Grizonnet, M.; Michel, J.; Poughon, V.; Inglada, J.; Savinaud, M.; Cresson, R. Orfeo ToolBox: Open source processing of remote sensing images. *Open Geospat. Data Softw. Stand.* **2017**, *2*, 15. [[CrossRef](#)]
64. Zeiler, M.D.; Fergus, R. Visualizing and Understanding Convolutional Networks. In *Computer Vision—ECCV 2014*; Fleet, D., Pajdla, T., Schiele, B., Tuytelaars, T., Eds.; Springer Nature: Cham, Switzerland, 2014; pp. 818–833. ISBN 978-3-319-10589-5.
65. Schultz, M.; Voss, J.; Auer, M.; Carter, S.; Zipf, A. Open land cover from OpenStreetMap and remote sensing. *Int. J. Appl. Earth Obs. Geoinf.* **2017**, *63*, 206–213. [[CrossRef](#)]
66. Li, H.; Zech, J.; Ludwig, C.; Fendrich, S.; Shapiro, A.; Schultz, M.; Zipf, A. Automatic mapping of national surface water with OpenStreetMap and Sentinel-2 MSI data using deep learning. *Int. J. Appl. Earth Obs. Geoinf.* **2021**, *104*, 102571. [[CrossRef](#)]
67. Gillhaus, K.; Boch, S.; Fischer, M.; Hölzel, N.; Kleinebecker, T.; Prati, D.; Rupprecht, D.; Schmitt, B.; Klaus, V.H. Grassland management in Germany: Effects on plant diversity and vegetation composition. *Tuexenia* **2017**, *37*, 379–397. [[CrossRef](#)]
68. Peringer, A.; Schulze, K.A.; Giesbrecht, E.; Stanik, N.; Rosenthal, G. *“Wildes Offenland“: Bedeutung und Implementierung von “Störungen“ für den Erhalt von Offenlandökosystemen in ansonsten nicht gemanagten (Schutz-)Gebieten; Abschlussbericht des gleichnamigen F+E-Vorhabens (FKZ 3515 85 0500, Laufzeit 10/2015 bis 12/2017)*, 2nd ed.; Bundesamt für Naturschutz: Bonn-Bad, Godesberg, 2019.
69. Blüthgen, N.; Dormann, C.F.; Prati, D.; Klaus, V.H.; Kleinebecker, T.; Hölzel, N.; Alt, F.; Boch, S.; Gockel, S.; Hemp, A.; et al. A quantitative index of land-use intensity in grasslands: Integrating mowing, grazing and fertilization. *Basic Appl. Ecol.* **2012**, *13*, 207–220. [[CrossRef](#)]
70. Robbins, P. Beyond Ground Truth: GIS and the Environmental Knowledge of Herders, Professional Foresters, and Other Traditional Communities. *Hum. Ecol.* **2003**, *31*, 233–253. [[CrossRef](#)]
71. Baka, J. What wastelands? A critique of biofuel policy discourse in South India. *Geoforum* **2014**, *54*, 315–323. [[CrossRef](#)]
72. Bryn, A.; Bekkby, T.; Rinde, E.; Gundersen, H.; Halvorsen, R. Reliability in Distribution Modeling—A Synthesis and Step-by-Step Guidelines for Improved Practice. *Front. Ecol. Evol.* **2021**, *9*, 658713. [[CrossRef](#)]
73. Fernandes, R.F.; Scherrer, D.; Guisan, A. Effects of simulated observation errors on the performance of species distribution models. *Divers. Distrib.* **2019**, *25*, 400–413. [[CrossRef](#)]

74. Chefaoui, R.M.; Lobo, J.M. Assessing the effects of pseudo-absences on predictive distribution model performance. *Ecol. Model.* **2008**, *210*, 478–486. [[CrossRef](#)]
75. Wisz, M.S.; Guisan, A. Do pseudo-absence selection strategies influence species distribution models and their predictions? An information-theoretic approach based on simulated data. *BMC Ecol.* **2009**, *9*, 8. [[CrossRef](#)]
76. Konvicka, M.; Hula, V.; Fric, Z. Habitat of pre-hibernating larvae of the endangered butterfly *Euphydryas aurinia* (Lepidoptera: Nymphalidae): What can be learned from vegetation composition and architecture? *Eur. J. Entomol.* **2003**, *100*, 313–322. [[CrossRef](#)]
77. Smee, M.; Smyth, W.; Tunmore, M.; French-Constant, R.; Hodgson, D. Butterflies on the brink: Habitat requirements for declining populations of the marsh fritillary (*Euphydryas aurinia*) in SW England. *J. Insect Conserv.* **2011**, *15*, 153–163. [[CrossRef](#)]
78. Betzholtz, P.-E.; Ehrig, A.; Lindeborg, M.; Dinnéztz, P. Food plant density, patch isolation and vegetation height determine occurrence in a Swedish metapopulation of the marsh fritillary *Euphydryas aurinia* (Rottentburg, 1775) (Lepidoptera, Nymphalidae). *J. Insect Conserv.* **2007**, *11*, 343–350. [[CrossRef](#)]
79. Guisan, A.; Edwards, T.C.; Hastie, T. Generalized linear and generalized additive models in studies of species distributions: Setting the scene. *Ecol. Model.* **2002**, *157*, 89–100. [[CrossRef](#)]
80. Pourtaghi, Z.S.; Pourghasemi, H.R.; Aretano, R.; Semeraro, T. Investigation of general indicators influencing on forest fire and its susceptibility modeling using different data mining techniques. *Ecol. Indic.* **2016**, *64*, 72–84. [[CrossRef](#)]
81. Kosicki, J.Z. Generalised Additive Models and Random Forest Approach as effective methods for predictive species density and functional species richness. *Environ. Ecol. Stat.* **2020**, *27*, 273–292. [[CrossRef](#)]
82. Opper, S.; Meirinho, A.; Ramírez, I.; Gardner, B.; O’Connell, A.F.; Miller, P.I.; Louzao, M. Comparison of five modelling techniques to predict the spatial distribution and abundance of seabirds. *Biol. Conserv.* **2012**, *156*, 94–104. [[CrossRef](#)]
83. Rew, J.; Cho, Y.; Moon, J.; Hwang, E. Habitat Suitability Estimation Using a Two-Stage Ensemble Approach. *Remote Sens.* **2020**, *12*, 1475. [[CrossRef](#)]
84. Mugo, R.; Saitoh, S.-I. Ensemble Modelling of Skipjack Tuna (*Katsuwonus pelamis*) Habitats in the Western North Pacific Using Satellite Remotely Sensed Data: a Comparative Analysis Using Machine-Learning Models. *Remote Sens.* **2020**, *12*, 2591. [[CrossRef](#)]
85. Zhang, C.; Wei, S.; Ji, S.; Lu, M. Detecting Large-Scale Urban Land Cover Changes from Very High Resolution Remote Sensing Images Using CNN-Based Classification. *ISPRS Int. J. Geo-Inf.* **2019**, *8*, 189. [[CrossRef](#)]
86. Zhang, X.; Han, L.; Han, L.; Zhu, L. How Well Do Deep Learning-Based Methods for Land Cover Classification and Object Detection Perform on High Resolution Remote Sensing Imagery? *Remote Sens.* **2020**, *12*, 417. [[CrossRef](#)]
87. Neyns, R.; Canters, F. Mapping of Urban Vegetation with High-Resolution Remote Sensing: A Review. *Remote Sens.* **2022**, *14*, 1031. [[CrossRef](#)]

Disclaimer/Publisher’s Note: The statements, opinions and data contained in all publications are solely those of the individual author(s) and contributor(s) and not of MDPI and/or the editor(s). MDPI and/or the editor(s) disclaim responsibility for any injury to people or property resulting from any ideas, methods, instructions or products referred to in the content.